Intercalation of Conducting Poly(*N*-propane sulfonic acid aniline) in V_2O_5 Xerogel

Jing Zhao, Gengchao Wang, Xingwei Li, Chunzhong Li

Key Laboratory for Ultrafine Materials of Ministry of Education, School of Materials Science and Engineering, East China University of Science and Technology, Shanghai 200237, People's Republic of China

Received 18 April 2006; accepted 17 July 2006
DOI 10.1002/app.25141
Published online in Wiley InterScience (www.interscience.wiley.com).

ABSTRACT: Poly(*N*-propane sulfonic acid aniline) (PSPAN) can be formed between the lamellas of V_2O_5 xerogel by *in situ* oxidative polymerization/intercalation of *N*-propane sulfonic acid aniline in the presence of air (V_2O_5 being the oxidation agent). The PSPAN/V_2O_5 nanocomposites were characterized by XRD, TEM, TGA, FTIR, UV–vis-NIR, and conductivity measurement. The results show that the V_2O_5 maintains lamellar structure, but its interlayer spacing has increased from 1.18 to 1.31 nm. The FTIR spectra indicate that there is interaction between negatively charged oxygen of the sulfonic group of PASPN and the vanadium ion in V_2O_5 matrix. The electrical conductivity of PSPAN/V_2O_5 nanocomposite reached the value of 1.2×10^{-2} S/cm, which is 10^4 times higher than that of the V_2O_5 xerogel, and is 10^2 times more than that of the PSPAN. It was found that the aging in air facilitated the chain growth of PSPAN between the V_2O_5 lamellas, resulting in the increase of the electrical conductivity. © 2006 Wiley Periodicals, Inc. J Appl Polym Sci 103: 2569–2574, 2007

Key words: conducting polymer; V_2O_5 xerogel; nanocomposites; intercalation

INTRODUCTION

Researchers have extensively investigated the nanocomposites formed from transition metal oxides and electronically conducting polymers, which can be used in many fields, such as rechargeable lithium batteries, electrochromic display devices, and humidity sensors.[1–4] V_2O_5 xerogel's distinctive two-dimensional layered structure and high specific capacity make it a potentially excellent cathode material used in secondary lithium batteries.[5–7] However, V_2O_5 xerogel shows some drawbacks such as low electrical conductivity, poor structural stability resulted from the electrochemical intercalation/deintercalation of Li^+, and high variability of the coordination geometry at the metal center.[8,9]

To address the issues mentioned earlier, several conducting polymers including polyaniline,[4,7,10–13] polypyrrole,[14–16] polythiophene,[17,18] and poly(ethylene oxide)[3,19] have been introduced. The intercalation of conducting polymers can not only improve the poor electrical conductivity of V_2O_5 xerogel, but also maintain the layered structure of V_2O_5 xerogel.

Conducting sulfonated polyaniline/V_2O_5 nanocomposites have also been synthesized using sol–gel method[9] by simply mixing sulfonated polyaniline aqueous solution with V_2O_5 wet gel.[20] The main advantage of using these conducting polymers would be the possibility of maximizing the transport number for Li^+ by minimizing the participation of anions induced by the electrostatic repulsion between the sulfonic groups.[21] In this article, we report a method to synthesize a poly(*N*-propane sulfonic acid aniline)/V_2O_5 nanocomposite. In this method, *N*-propane sulfonic acid aniline is first intercalated into V_2O_5 xerogel host, and then converted into poly(*N*-propane sulfonic acid aniline) through *in situ* polymerization oxidized by V_2O_5 in the presence of air. After being aged in air, the poly(*N*-propane sulfonic acid aniline)/V_2O_5 nanocomposite synthesized has a relatively high electrical conductivity (1.2×10^{-2} S/cm).

EXPERIMENTAL

Materials

Aniline of analytical grade was purchased from Shanghai Chemical Reagent and distilled under vacuum prior to use. 1,3-Propane sultone (Kyoto Kaisei Kogyo), crystalline V_2O_5 powder, 30% hydrogen peroxide (H_2O_2) solution, and all other reagents were received as analytical grades, and were used without further purification.

Correspondence to: G. Wang (gengchaow@ecust.edu.cn).
Contract grant sponsor: National Natural Science Foundation of China; contract grant number: 20236020.
Contract grant sponsor: Shanghai Municipal Science and Technology Commission; contract grant numbers: 04DZ14002, 0352nm052.

Journal of Applied Polymer Science, Vol. 103, 2569–2574 (2007)

Preparation of V_2O_5 xerogel

V_2O_5 xerogel was prepared following the previously reported sol–gel method.[22] A 5 g of V_2O_5 crystalline powder was dissolved in 120 mL of 10% hydrogen peroxide aqueous solution under agitation at ambient temperature. An orange solution was formed after about 10 min, and this solution was turned into a dark-red gel after 48 h. The dark-red gel was cast onto a glass substrate and aged for 1 month. The aged gel was then heated to 120°C, and then treated at this temperature for 4 h to give the $V_2O_5{\cdot}nH_2O$ xerogel.

Sythesis of *N*-propane sulfonic acid aniline

N-propane sulfonic acid aniline (SPAN) was synthesized according to the previous described method.[9] Aniline (2.0 g, 21.5 mmol) and 1,3-propane sultone (5.2 g, 43.0 mmol) were added together into 20 mL of ethanol. The reaction was allowed to proceed for 24 h at 60°C. The white precipitate obtained was purified with recrystallization method. The FTIR spectrum of this sample showed the following bands: 3400–3500 cm^{-1} (N—H stretching), 2850–2900 cm^{-1} (aliphatic C—H stretching), 1500 cm^{-1} (C=C benzenoid stretching), 1310 cm^{-1} (C—N secondary aryl amine bending), 1160 cm^{-1} (S=O asymmetric stretching), 1030 cm^{-1} (S=O symmetric stretching), and 820 cm^{-1} (C—H out of plane bending). The elemental analysis indicated S/N molar ratio of 1. These measurements reveal the structure and of *N*-propane sulfonic acid aniline.

Synthesis of bulk poly[*N*-propane sulfonic acid aniline]

SPAN (2.0 g, 9.3 mmol) was first dissolved in 50 mL of deionized water, and then 2.1 g (9.3 mmol) of ammonium persulfate (dissolved in 25 mL of deionized water) was dropped into the above-mentioned solution. The polymerization was allowed to proceed for 24 h at 0–5°C. The dark-green solution was dialyzed for 3 days using dialysis membrane (molecular weight cutoff, 3500) in deionized water, which was replaced with fresh deionized water frequently, to remove salts and oligomers. The resulting solution was dried at 70°C to produce the bulk poly[*N*-propane sulfonic acid aniline] (PSPAN) powder.

Synthesis of PSPAN/V_2O_5 nanocomposite

SPAN (2.0 g) was dissolved in the 50 mL of deionized water, and then added into 2.0 g of V_2O_5 xerogel dispersed in 25 mL of deionized water. After being stirred at 0–5°C for 24 h, the dark-green precipitate was isolated by filtration, aged in air for various times, washed with deionized water to remove the residual PSPAN present on the surface, and finally dried in vacuum.

Extraction of PSPAN from PSPAN/V_2O_5

PSPAN/V_2O_5 (0.2 g) was dissolved in 50 mL of 1*M* NaOH (aq), then dialyzed using dialysis membrane (molecular weight cutoff, 3500) in deionized water to remove the inorganic components. The resulting solution was dried at 70°C to give extracted PSPAN.

Measurements

X-ray diffraction (XRD) patterns were observed with a Rigaku D/Max 2550 VB/PC X-ray diffractometer using Cu Kα radiation. The diffraction data were recorded for 2θ angles between 3° and 60°. Transmission electron microscopy (TEM) was carried out using a JEM-2010 instrument operated at 200 kV. The samples for TEM were prepared by ultrasonically distributing powder in ethanol and coating very little amount of this solution onto wholly carbon-coated copper grids. FTIR spectra were recorded from KBr pellets using a Nicolet AVATAR360 spectrometer. Thermogravimetric analyses (TGA) were preformed on a TGA/SDTA/851e thermogravimetric analyzer running from room temperature to 600°C at a heating rate of 5°C/min under air. UV–vis-NIR spectra of the samples were recorded on a Varian Cary 500 Scan NIR spectrophotometer. The electrical conductivity of the samples was determined by four-probe method using compressed pellets and a SX 1934 four-probe instrument.

RESULTS AND DISCUSSION

Reaction of SPAN with V_2O_5 xerogel

The steps of the intercalative polymerization of SPAN in the V_2O_5 are presented schematically in Scheme 1. The intercalation of SPAN in V_2O_5 xerogel is a redox reaction in which SPAN is oxidized and V_2O_5 is reduced. First, SPAN was diffused into the V_2O_5 interlayer space and converted into the SPAN cations in the acidic environment of V_2O_5 interlayers. Then, the SPAN cations are oxidized by V_2O_5, resulting in PSPAN oligomer formation. The reduced V_2O_5 was reoxidized by the oxygen in the air. When the samples are aged in air, the SPAN oligomers inside the V_2O_5 gallery further condense to form longer chain polymers. The effect of aging on the length of the PSPAN chains was investigated using dialyzed extraction experiments. When the freshly prepared PSPAN/V_2O_5 was dissolved in 1*M* NaOH solution and dialyzed by dialysis membrane (molecular weight cutoff; 14,000) in deionized water, the

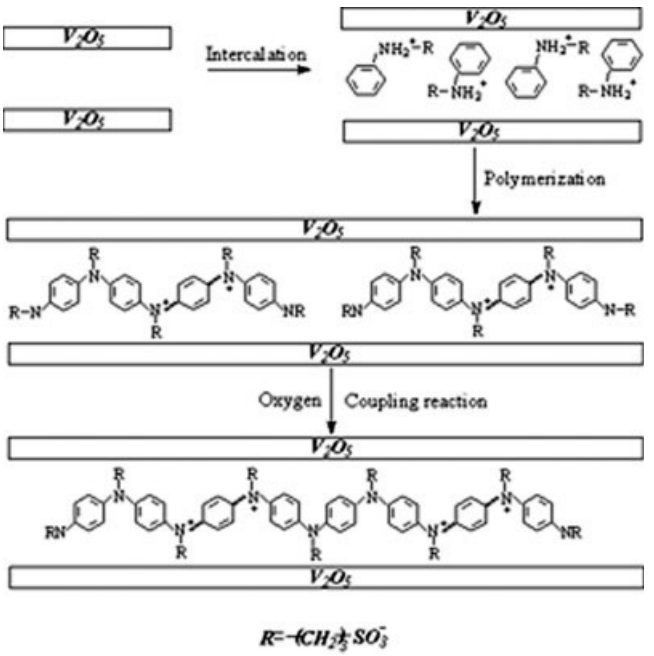

Scheme 1 Schematic illustration for formation of PSPAN intercalated V_2O_5 xerogel.

PSPAN residue was not observed in the dried solution obtained. In contrast, in the 2 months aged PSPAN/V_2O_5 sample treated by the same processes, the PSPAN polymer was detected, indicating that long chain PSPANs were formed during the aging.

Micromorphology

Figure 1 shows X-ray diffraction patterns of bulk PSPAN, V_2O_5 xerogel, and PSPAN/V_2O_5. The curve of bulk PSPAN exhibits a wide and diffuse reflection at $2\theta = 20^\circ$, which indicates that bulk PSPAN is an amorphous structure [Fig. 1(a)]. The pattern of V_2O_5 xerogel shows a stronger (001) peak, which is a typical property of a quasi-crystalline layered material [Fig. 1(b)]. The 2θ value corresponds to an interlayer spacing of 1.18 nm, which is consistent with the previous report.[23] The (001) diffraction peak for PSPAN/V_2O_5 shifts to a lower angle, and the interlayer spacing of PSPAN/V_2O_5 expands to 1.31 nm from 1.18 nm of V_2O_5 xerogel [Fig. 1(c)]. The expansions of spacing suggest that at least a fraction of PSPAN chain intercalate into the lamella of V_2O_5, indicating that the PSPAN chain is parallel to (001) plane, and an intimate contact exists between the conducting PSPAN and the host matrix. The PSPAN containing V_2O_5 matrix is a nanocomposite. The weak (001) reflection for PSPAN/V_2O_5 shows a poorly organized structure when compared with V_2O_5.[24]

Figure 2 shows the transmission electron micrographs of V_2O_5 xerogel and PSPAN/V_2O_5 nanocomposite. In these figures, the gray strips stand for the V_2O_5 layers, while the black strips represent for the spaces between the layers. The TEM micrographs reveal that both the samples before and after the PSPAN intercalation have layered structures. It is also found that the space between the layers increases with the intercalation of PSPAN into the V_2O_5 xerogel. The repeated distances (1–2 nm) from the TEM micrographs are in good agreement with the *d* spacing provided by XRD.

Thermogravimetric analysis

Figure 3 gives thermogravimetric analysis (TGA) curves for bulk PSPAN, V_2O_5 xerogel, and PSPAN/V_2O_5 nanocomposite. The thermogravimetric curve of bulk PSPAN shows two main weight losses [Fig. 3(a)]. The first weight loss below ca. 200°C corresponds to the small weight loss of water and oligomers. The considerable weight loss between ca. 200°C and ca. 580°C is attributed to the decomposition of PSPAN. The thermogravimetric curve of V_2O_5 xerogel also shows two weight losses [Fig. 3(b)]. The first weight loss (ca. 9%) below ca. 120°C is attributed to the removal of the weakly bounded water from the V_2O_5 interlayer region. The second weight loss (ca. 2%) extends up to ca. 280°C, which corresponds to the removal of the strongly bonded water.

For the PSPAN/V_2O_5 nanocomposite, the two distinct weight losses are visible [Fig. 3(c)]. The first weight loss extends to ca. 120°C corresponds to the loss of noncoordinated water from the interlamella, indicating that the PSPAN/V_2O_5 nanocomposite contains ca. 6% water. In the second step, substantial weight loss between ca. 120°C and ca. 415°C is assigned to the combustion of the organic component, which can be used to confirm the PSPAN content in

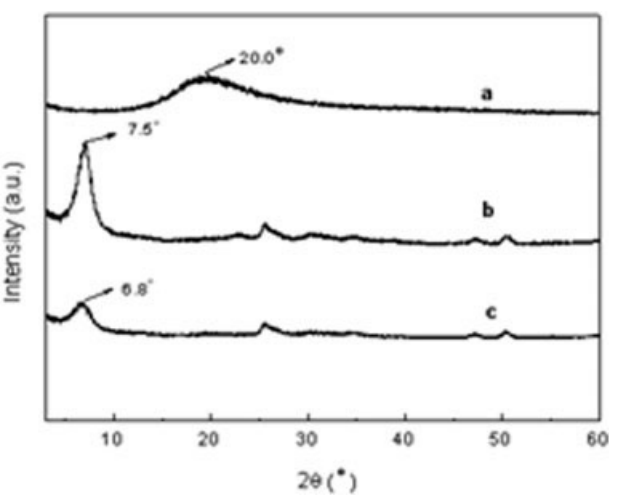

Figure 1 XRD patterns of (a) bulk PSPAN, (b) V_2O_5 xerogel, and (c) PSPAN/V_2O_5.

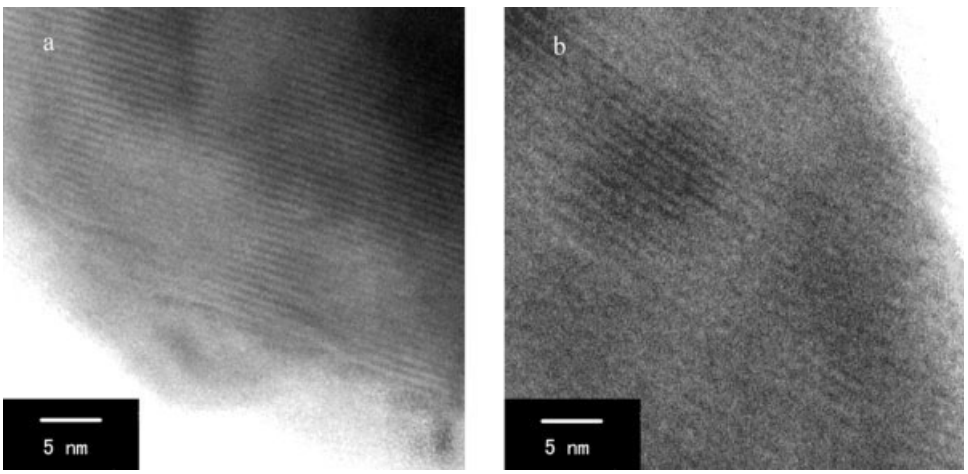

Figure 2 Transmission electron micrographs of (a) V_2O_5 xerogel and (b) PSPAN/V_2O_5.

the nanocomposite with the value of ca. 19%, and the loss of strongly bonded water. The latter is too small and can be neglected. The distinct mass gain that occurs between 415 and 425°C is ascribed to the oxygen absorption by the V^{4+} centers in the inorganic lattice, which was sacrificed during reductive intercalative coupling of the monomer to form the PSPAN. Moreover, the weight gain can be used to determine δ [$\delta = V^{4+}/(V^{4+} + V^{5+})$]. The chemical composition of the nanocomposite determined by TGA is $[PSPAN]_{0.25}V_2O_{5-\delta}{\cdot}0.92H_2O$ ($\delta = 0.14$).

Fourier transform infrared spectra

Figure 4 shows the FTIR spectra of bulk PSPAN, V_2O_5 xerogel, PSPAN/V_2O_5 nanocomposite, and the PSPAN extracted from PSPAN/V_2O_5. For the bulk PSPAN [Fig. 4(a)], the absorption bands at 1573 and 1501 cm^{-1} are attributed to C=C stretching vibrations of the quinoid and benzenoid rings. The absorption bands at 1140 and 1033 cm^{-1} are assigned to the asymmetric and symmetric O=S=O stretching vibrations. The band at 821 cm^{-1} is associated to the C—H out-of-plane bending vibration of 1,4-disubstituted benzene rings.

The characteristic bands of V_2O_5 xerogel are clearly observed in Figure 4(c). The three bands at 1005, 763, and 526 cm^{-1} are assigned to the stretching of

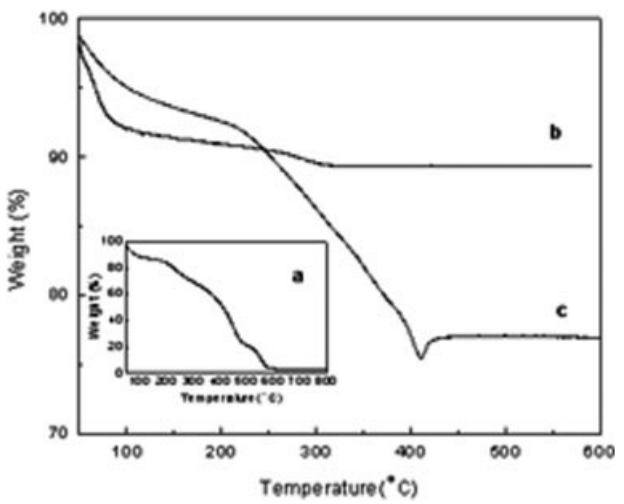

Figure 3 TGA curves of (a) bulk PSPAN, (b)V_2O_5 xerogel, and (c) PSPAN/V_2O_5.

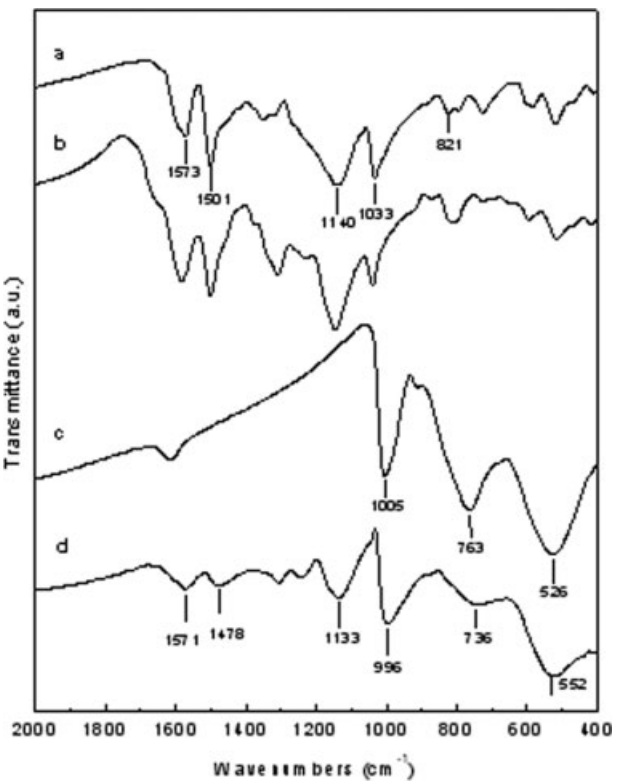

Figure 4 FTIR spectra of (a) bulk PSPAN, (b) extracted PSPAN from PSPAN/V_2O_5, (c) V_2O_5 xerogel, and (d) PSPAN/V_2O_5.

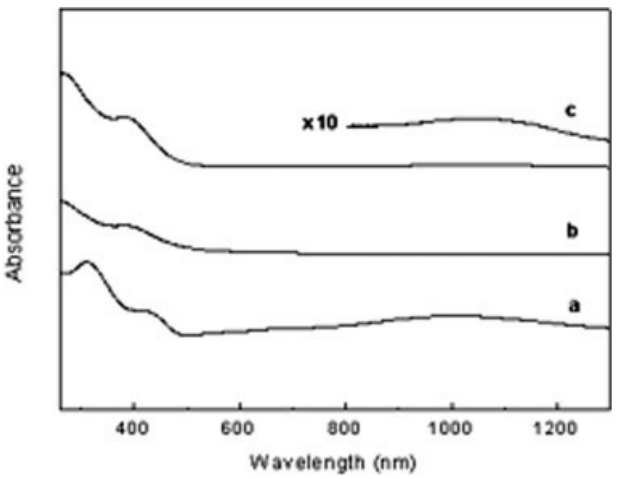

Figure 5 UV–vis-NIR spectra of (a) bulk PSPAN, (b) PSPAN/V_2O_5 hybrid, and (c) PSPAN/V_2O_5 mixture.

V=O, and the asymmetric and symmetric stretching of V—O—V,[25] respectively.

Figure 4(d) shows the FTIR spectrum obtained for the nanocomposite. The presence of PSPAN is evidenced through the bands above 1010 cm^{-1}. The bands at 1571 and 1478 cm^{-1} are assigned to C=C stretching for the benzenoid and quinoid rings in PSPAN, which is shifted toward red band when compared with Figure 4(a). This is because the PSPAN chain change from curly chains conformation to outstretched chain conformation in a constrained environment, which improves the conjugation degree of PSPAN chains.[26] The band at 1133 cm^{-1} corresponding to the asymmetric S=O stretch in PSPAN/V_2O_5 nanocomposite shifts to lower wave numbers, indicating that there is interaction between negatively charged oxygen of the sulfonic group and the vanadium ion. In addition, the characteristic bands corresponding to V_2O_5 material are clearly observed in Figure 4(d). This implies that the 2D layer structure of V_2O_5 has not been destroyed by intercalation of PSPAN.

From Figure 4(a,b), it is found that the FTIR spectrum of the PSPAN extracted from PSPAN/V_2O_5 is very similar to that of bulk PSPAN, which indicates that the PSPAN is formed through the oxidation of SPAN by V_2O_5.

UV–vis-NIR spectra analysis

Figure 5(a) shows that the absorption peak at 800–1000 nm corresponds to the localized polaron transition of bulk PSPAN. For PSPAN/V_2O_5 mixture, the absorption peak at 800–1000 nm has also appeared [Fig. 5(c)]. However, for PSPAN/V_2O_5 hybrid nanocomposite, the absorption peak at 800–1000 nm assigning to the localized polaron transition of the PSPAN disappears, which indicate that the PSPAN chains have expanded coil-like conformation.[27] The XRD result also indicates that the PSPAN exist in chains with extended-chain conformations owing to the confined space in the nanometer-size gallery.

Electrical properties

PSPAN and V_2O_5 xerogel are both electrically conducting materials. There are two types of charge carriers in PSPAN/V_2O_5 nanocomposite, one of which is electron associated with the d^1 (V^{4+}) centers found on the vanadium oxide lattice and the other of which is massive polaron located on the backbones of PSPAN. Therefore, the electrical conductivity in PSPAN/V_2O_5 should depend on the relative mobility of the two different kinds of carriers.

The variable-temperature electrical conductivity plots of PSPAN/V_2O_5, bulk PSPAN, and V_2O_5 xerogel are shown in Figure 6. The electrical conductivity of all samples increases with temperature, a characteristic of thermally activated behavior, due to interparticle contact resistance. This behavior has also been observed in polyaniline[28] and V_2O_5 xerogel.[29] The electrical conductivity of PSPAN/V_2O_5 is 10^4 times higher than that of V_2O_5 xerogel and 10^2 times more than that of PSPAN. The higher conductivity of PSPAN/V_2O_5 when compared with these of PSPAN, and V_2O_5 should result from the cooperation effect between two electric conducting materials, PSPAN and V_2O_5.[20] In PSPAN/V_2O_5, PSPAN and V_2O_5 closely contact and the charges can be transported between them through the polymer chains or the V_2O_5 framework. The mobility of the charge carriers is better than these in PSPAN or in V_2O_5. Moreover, the existence of PSPAN with extended-chain conformation in V_2O_5 gallery improves the conductivity.

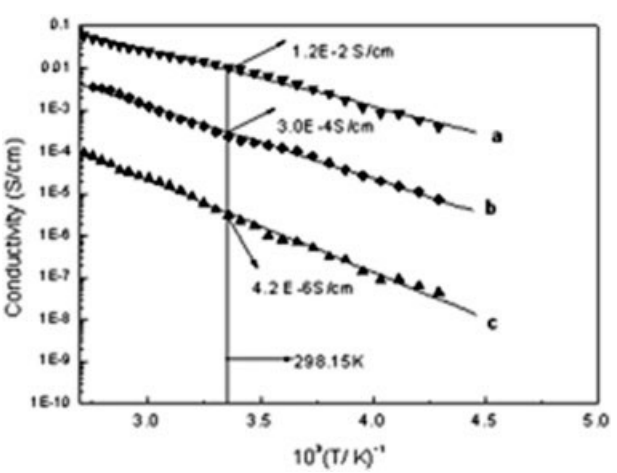

Figure 6 Variable-temperature electrical conductivity plots of pellets (a) PSPAN/V_2O_5, (b) bulk PSPAN, and (c) V_2O_5 xerogel.

TABLE I
The Electrical Conductivity of V_2O_5 Xerogel and PSPAN/V_2O_5 After Various Aging Times

Samples	Conductivity (S/cm)
V_2O_5 xerogel	4.2×10^{-6}
PSPAN	3.0×10^{-4}
Freshly prepared PSPAN/V_2O_5	5.9×10^{-4}
PSPAN/V_2O_5 aged 1 week	2.0×10^{-3}
PSPAN/V_2O_5 aged 1 month	3.7×10^{-3}
PSPAN/V_2O_5 aged 2 months	1.2×10^{-2}

The conductivity of the PSPAN/V_2O_5 nanocomposite is expected to be influenced by the polymer content, chain conformation, and chain length (MW). Table I shows that the electrical conductivity of the freshly prepared PSPAN/V_2O_5 nanocomposite is 5.9×10^{-4} S/cm^{-1}, and the conductivity of the aged nanocomposite increases with the aging time. The conductivity reached 1.2×10^{-2} S/cm after 2-month aging.

CONCLUSIONS

The PSPAN/V_2O_5 nanocomposites were synthesized by *in situ* oxidative polymerization and intercalation of *N*-propane sulfonic acid aniline (SPAN) in the galleries of the V_2O_5. The XRD and TEM studies show that SPAN is intercalated into the V_2O_5 matrix without damaging the lamellar structure. The FTIR results indicate that there is bonding interaction between negatively charged oxygen of the organic component, and the vanadium ion of the inorganic component. The conductivity of the freshly prepared PSPAN/V_2O_5 nanocomposite is 10^2 times higher than that of the V_2O_5 xerogel. Aging of the nanocomposites in air leads to the oxidative coupling of the PSPAN inside the interlamellar space, which results in the formation of the longer PSPAN chains and higher electrical conductivity. The conductivity of PSPAN/V_2O_5 nanocomposite increased with the aging time under air, and reached the value of 1.2×10^{-2} S/cm after 2 months. Our results have indicated the formation of a new hybrid material instead of a simple physical mixture of the starting material.

References

1. Cheetham, A. K. Science 1994, 264, 794.
2. Oliveira, H. P.; Graeff, C. F. O.; Brunello, C. A.; Guerra, E. M. J Noncryst Solids 2000, 273, 193.
3. Chen, W.; Xu, Q.; Hu, Y. S.; Mai, L. Q.; Zhu, Q. Y. J Mater Chem 2002, 12, 1926.
4. Huguenin, F.; Ferreira, M.; Zucolotto, V.; Nart, F. C.; Torresi, R. M.; Oliveira, O. N. Chem Mater 2004, 16, 2293.
5. Livage, J. Chem Mater 1991, 3, 578.
6. Lira-Cantú, M.; Gomez-Rómeto, P. J Electrochem Soc 1999, 146, 2029.
7. Wu, C.; DeGroot, D. C.; Marcy, H. O.; Schindler, J. L.; Kannewurf, C. R.; Liu, Y. J.; Hirpo, W.; Kanatzidis, M. G. Chem Mater 1996, 8, 1992.
8. Park, H. K.; Smyrl, W. H.; Ward, M. D. J Electrochem Soc 1995, 142, 1068.
9. Huguenin, F.; Gambardella, M. T. P.; Torresi, R. M.; Torresi, S. I. C.; Buttry, D. A. J Electrochem Soc 2000, 147, 2437.
10. Liu, Y. J.; DeGroot, D. C.; Schindler, J. L.; Kannewurf, C. R.; Kanatzidis, M. G. J Chem Soc Chem Commum 1993, 7, 593.
11. Gomez-Romero, P. Adv Mater 2001, 13, 163.
12. Li, Z. F.; Ruckenstein, E. Langmuir 2002, 18, 6956.
13. Ferreira, M.; Huguenin, F.; Zucolotto, V.; Silva, J. E. P.; Torresi, S. I. C.; Temperini, M. L. A.; Torresi, R. M.; Oliveira, O. N. J Phys Chem B 2003, 107, 8351.
14. Maia, G.; Torresi, R. M.; Ticianelli, E. A.; Nart, F. C. J Phys Chem 1996, 100, 15910.
15. Wong, H. P.; Dave, B. C.; Leroux, F.; Harreld, J.; Dunn, B.; Nazar, L. F. J Mater Chem 1998, 8, 1019.
16. Kuwabata, S.; Masui, S.; Tomiyori, H.; Yoneyama, H. Electrochem Acta 2000, 46, 91.
17. Goward, G. R.; Leroux, F.; Nazar, L. F. Electrochim Acta 1998, 43, 1307.
18. Murugan, A. V.; Kwon, C. W.; Campet, G.; Kale, B. B.; Mandale, A. B.; Sainker, S. R.; Gopinath, C. S.; Vijayamohanan, K. J Phys Chem B 2004, 108, 10736.
19. Huguenin, F.; dos Santos, D. S.; Bassi, A.; Nart, F. C.; Oliveira, O. N. Adv Funct Mater 2004, 14, 985.
20. Wu, C. G.; Hwang, J. Y.; Hsu, S. S. J Mater Chem 2001, 11, 2061.
21. Huguenin, F.; Giz, J. M.; Ticianelli, E. A.; Torresi, R. M. J Power Sour 2001, 103, 113.
22. Alonso, B.; Livage, J. J Solid State Chem 1999, 148, 16.
23. Shouji, E.; Buttry, D. A. Langmuir 1999, 15, 669.
24. Wang, G. C.; Wang, L.; Li, X. W. Polym Int 2005, 54, 1082.
25. Leroux, F.; Goward, G.; Power, W. P.; Nazar, L. F. J Electrochem Soc 1997, 144, 3886.
26. Wang, G. C.; Yang, Z. Y.; Li, X. W.; Li, C. Z. Carbon 2005, 43, 2564.
27. MacDiarmid, A. G.; Chang, J. C.; Halpern, M.; Mu, W. L.; Somasiri, N. L. D.; Wu, W.; Yaniger, S. I. Mol Cryst Liq Cryst 1985, 121, 173.
28. Zuo, F.; Angelopoulos, M.; MacDiarmid, A. G.; Epstein, A. J. Phys Rev B 1987, 36, 3475.
29. Bullot, J.; Gallais, O.; Gauthier, M.; Livage, J. Appl Phys Lett 1980, 36, 986.